View metadata, citation and similar papers at core.ac.uk

brought to you by CORE

provided by ACMAC

ΠΑΝΕΠΙΣΤΗΜΙΟ ΚΡΗΤΗΣ - ΤΜΗΜΑ ΕΦΑΡΜΟΣΜΕΝΩΝ ΜΑΘΗΜΑΤΙΚΩΝ
Archimedes Center for Modeling, Analysis & Computation
UNIVERSITY OF CRETE - DEPARTMENT OF APPLIED MATHEMATICS
Archimedes Center for Modeling, Analysis & Computation

ACMAC

ACMAC's PrePrint Repository

A Molecular Dynamics Study of Polymer/Graphene Nanocomposites

Anastassia Rissanou and Vagelis Harmandaris

Original Citation:

Rissanou, Anastassia and Harmandaris, Vagelis

(2013)

A Molecular Dynamics Study of Polymer/Graphene Nanocomposites.

Journal of Macromolecular Symposia.

ISSN MS-Nr: masy.201300070.R1

(In Press)

This version is available at: http://preprints.acmac.uoc.gr/236/
Available in ACMAC's PrePrint Repository: July 2013

ACMAC's PrePrint Repository aim is to enable open access to the scholarly output of ACMAC.

http://preprints.acmac.uoc.gr/

A Molecular Dynamics Study of Polymer/Graphene Nanocomposites

Anastassia N. Rissanou[1,2] and Vagelis Harmandaris[1,2]*

[1]Department of Applied Mathematics, University of Crete, GR-71409, Heraklion, Crete, Greece.
[2]Archimedes Center for Analysis, Modeling & Computation, University of Crete, P.O. Box 2208, GR-71003, Heraklion, Greece.
[3]Institute of Applied and Computational Mathematics (IACM), Foundation for Research and Technology Hellas (FORTH), GR-71110 Heraklion, Crete, Greece.

Summary: Graphene based polymer nanocomposites are hybrid materials with a very broad range of technological applications. In this work, we study three hybrid polymer/graphene interfacial systems (polystyrene/graphene, poly(methyl methacrylate)/graphene and polyethylene/graphene) through detailed atomistic molecular dynamics (MD) simulations. Density profiles, structural characteristics and mobility aspects are being examined at the molecular level for all model systems. In addition, we compare the properties of the hybrid systems to the properties of the corresponding bulk ones, as well as to theoretical predictions.

Keywords: molecular dynamics, nanocomposites, graphene, polymer

Introduction

Graphene is a very important material with a wide range of novel applications due to it's exceptional physical properties[1]. For this reason graphene can be thought as a promising candidate for the amplification of polymer nanocomposites' properties, taking the position of carbon nanotubes[2]. Graphene polymer nanocomposites are based on the incorporation of graphene in polymer matrices. The benefits which have been reported, for the hybrid system, are the improvement of the electrical, thermal, mechanical and gas barrier properties of graphene-polymer composites[3].

Due to the above properties the study of graphene based polymer composite materials is a very intense research area. For example, many studies on the reinforcement of graphene – polymer nanocomposites have used either graphene oxide[4,5,6] or a single

* Author to whom correspondence should be addressed:
rissanou@tem.uoc.gr +30 2810393746 fax: +30 2810393701

atomic layer of exfoliated graphene. The former induces stronger adhesion between graphene and polymer.[7]

Besides experiments, simulation methodologies can also be used for the study of polymer/graphene hybrid nanostructured systems, providing a detailed investigation of the hybrid system, and especially of the interface, at the molecular level. For example, Harmandaris et al. and Daoulas et al.[8], in a series of two papers, reported on modeling of hybrid polymer/graphite systems, through state-of-the-art atomistic Monte Carlo (MC) and Molecular Dynamics (MD) simulations. Furthermore, Awasthi et al.[9], studied the graphene-polyethylene interfacial mechanical behavior using MD simulations. More recently, Lv et al.[10] performed a simulation study where the influence of the chemical functionalization of graphene on the interfacial bonding characteristics was presented.

In the current work we present results, which are a part of a general computational approach for the study of realistic polymer/graphene systems, with main goal the *quantitative prediction* of the macroscopic properties of realistic nanocomposite systems, especially at the interface. To achieve this, polymer/graphene hybrid systems are required to be examined at various length and time scales. Therefore, hierarchical multi scale methodologies, which involve systematic linking between simulation methods from different levels of description, are necessary[11,12]. Such simulation approaches are described via typical length-time graphs presenting the length and time range in which each simulation method is valid, as the one shown in Figure 1.[13] In more detail, in Figure 1 representative snapshots from polymer–solid interfacial systems from different levels of description (from the quantum level, through classical atomistic models, to coarse-grained models and up to continuum models), as well as, the corresponding simulation methods, are presented. Note that a rigorous and systematic procedure is required in order to link the different levels of description. The overall methodology will allow us to provide a fundamental study of the coupling between microstructure at the interface and macroscopic properties (structural, mechanical, elastic and dynamical-rheological) of graphene/polymer nanocomposite systems.

In the present study, we report data through all-atom classical simulations of hybrid systems consisted of graphene and three well known and widely used polymers; the atactic Polystyrene (PS), the atactic Poly(methyl-methacrylate) (PMMA) and Polyethylene (PE). We examine their structural and dynamical properties and detect the effect of the graphene

layer on them, through a comparison with the corresponding bulk systems' properties. Moreover, we make a comparison among the three different hybrid systems.

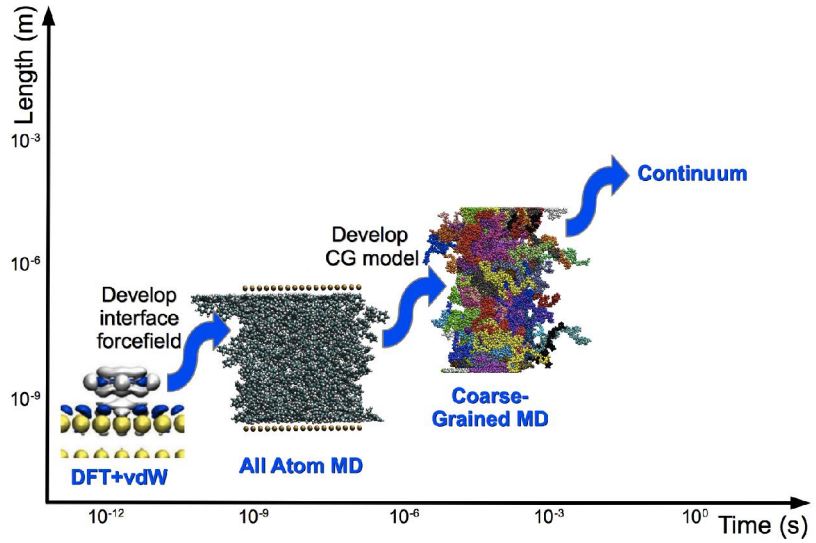

Figure 1. A schematic representation of the hierarchical simulation approach linking different levels of description[13].

Systems and Simulation Method

The systems studied in this work are depicted in Table 1. These are the following polymer/graphene composites: (a) PS/Graphene, (b) PMMA/Graphene and (c) PE/Graphene. The corresponding bulk polymer systems are studied as well. *N* is the number of polymer chains in the simulation box. For PS and PMMA polymer chains were *10*-mers, while PE chains consist of *22*-mers, (i.e. 22 CH_2 groups). Note that the molecular backbone length of all systems is very similar, since PS and PMMA chains have 20 (CH_2 or CH) groups in the backbone. The reference bulk systems consist of *56 10*-mer chains for PS, *54 10*-mer chains for PMMA and *420 22*-mer chains for PE. The film thickness (*d*), which is included in the third column of Table 1, is calculated from the box length along the *z*-direction subtracting the thickness of the graphene layer, (*0.34nm*, i.e. about one van der Waals radius), which is placed at *z=0*. The number and the length of the polymer chains in each system were chosen so that they form polymer films of almost equal thicknesses. The last three columns of Table 1 will be discussed in the next section.

We performed atomistic *NPT* and *NVT* Molecular Dynamics (MD) simulations using the GROMACS code.[14] All simulations were carried out at constant temperature equal to *T=500K* for PS and PMMA and *T=450K* for PE, and pressure *P=1atm*. We chose relatively high temperature values, in order to enhance the mobility of polymers so as to

study their dynamics, but at the same time temperatures where experiments can be performed. For both PS and PMMA *T=500K* is an appropriate value, which is almost equidistant from their glass transition temperatures (i.e. $T_g^{PS} \cong 360K$, and $T_g^{PMMA} \cong 380K$). For PE $T_g^{PE} \cong 190K$, is substantially smaller than the T_g values of the other two polymers and an equidistant temperature from T_g^{PE} would lead to temperature values where PE is crystallized (i.e., $T\sim [310\text{-}330]K$). Therefore, since the melting point of PE is about 410K, we chose *T=450K* for this system.

Table 1

Number of Chains, Film Thickness, Radius of Gyration, End-to-End Distance and Segmental Relaxation Time for the PS the PMMA and the PE systems.

System	*N*	*d(nm)*	*Rg(nm)*	*Ree(nm)*	τ_{seg}*(ns)*
PMMA	135	13.35	0.697±0.001	1.71±0.02	250.55±20.0
Bulk PMMA	54	-	0.695±0.001	1.70±0.02	64.15±10.0
PS	120	13.67	0.695±0.001	1.56±0.01	26.30±8.0
Bulk PS	56	-	0.696±0.001	1.54±0.01	10.91±3.0
PE	420	13.91	0.631±0.003	1.82±0.01	0.0083±0.002
Bulk PE	420	-	0.620±0.003	1.77±0.01	0.0044±0.001

An all atom representation model has been used. For the description of the intermolecular and intramolecular interactions of PMMA and PS we have used the OPLS[15] atomistic force field, while for PE the TRaPPE model[16] has been used. For the interaction between polymer atoms and graphene layers the geometric means $\varepsilon_{ij} = (\varepsilon_{ii}\varepsilon_{jj})^{0.5}$ and $\sigma_{ij} = (\sigma_{ii}\sigma_{jj})^{0.5}$ were used with: $\varepsilon_{cc}/k_B=28K$ and $\sigma_{cc}=3.4Å$. The set of ε and σ values for the graphene carbons are the ones used by Steel[17], optimized for a basal plane of graphite. Graphene has been represented as a set of LJ carbon atoms, centered at their crystallographic positions. The lattice constant which has been used is that of graphite at *300K*, equal to *2.462Å*. Periodic boundary conditions have been used in all three directions, so that the polymer interacts with the graphene layer, which was placed at the bottom of the simulation box, on the *xy* plane, and its periodic image at the top of the simulation box simultaneously. This setup renders our systems polymer films confined between two graphene surfaces, i.e. assuming ideal dispersion of graphene sheets. This is

certainly not the usual case for realistic nanocomposites[18], however we do not expect this assumption to introduce artifacts, since we are particular interested in large (compared to chain size) graphene layers and short time dynamics in which the motion of the layers is not important. The dimensions of the graphene sheets (i.e. *xy*-direction) in the simulation box are [*5.5-7.5*] times larger than the radius of gyration of the respective polymer chains. Nevertheless, periodic boundary conditions ensure an infinite graphene layer with no edges, which is eclectically neutral. More details about the all-atom force field, as well as the MD simulations are given elsewhere[19]. The *NPT* simulations of bulk systems provide a density of $0.965 g/cm^3$ for the PS, $1.054 g/cm^3$ for the PMMA and $0.663 g/cm^3$ for the PE.

Results

We start the discussion of the simulation results by calculating the chain dimensions. In Table 1 both the average radius of gyration, $\langle R_g \rangle$, and the end-to-end distance, $\langle R_{ee} \rangle$, are presented for all systems studied here. The values of the corresponding bulk systems are also included. PS and PMMA have almost equal radius of gyration, while the end-to-end distance of PS is smaller than the one of PMMA. For PE, $\langle R_g \rangle$ is lower, though $\langle R_{ee} \rangle$ is higher, compared to the other two polymers. An interesting observation is that the values of both $\langle R_g \rangle$ and $\langle R_{ee} \rangle$ are almost equal between the bulk and the confined systems respectively, except for PE, where the bulk system has a rather lower $\langle R_g \rangle$ and $\langle R_{ee} \rangle$ value, compared to the confined one.

The polymer arrangement, with respect to the surface, is presented through the calculation of the density profiles as a function of the distance from the graphene layer, $\rho(r)$. In Figure 2 three density profiles are depicted for the three hybrid polymer/graphene systems. Density profiles are based on the monomer center of mass and are averaged over time. There are common characteristic in all three cases: (a) An attraction of the polymer atoms from the graphene layer, which is denoted by the high peak (maximum) in the density curves. (b) The density profiles are, as expected, symmetrical with respect to the center of the film, due to the specific setup. (c) All three polymers attain their bulk density, almost in the middle of the polymer film. The bulk density value is presented with a dashed horizontal line in each system.

Although the qualitative picture is almost the same, for the three hybrid systems, a more careful observation brings out quantitative differences. The highest attraction from the surface is exerted on PS, PMMA follows, while the lowest is the one on PE, as it is

obvious from the values of the peaks in the density profiles. This can be attributed to: (a) the existence of a side group in the first two polymers (i.e., a phenyl ring in PS, a carboxyl and a methyl side group in PMMA), and (b): the fact that the polymer/graphene dispersion (van der Waals) forces are larger for PS and PMMA than for PE, because of their larger bulk density, i.e. there are more polymer atoms per unit volume. Moreover, graphene layer seems to prefer the phenyl ring more than the side groups of PMMA, which is reflected in the higher first peak of $\rho(r)$ for PS compared to PMMA. Another interesting observation is that PE, due to the absence of a side group, appears a more well ordered layered structure close to the surface, as it is evident from the second and the third peak in the density profile. The peaks become gradually lower as the distance from the surface increases (i.e. the attraction is smaller). On the contrary, a very small second peak is rather detectable in PS density profile, whereas the curve is structureless after the first peak in PMMA.

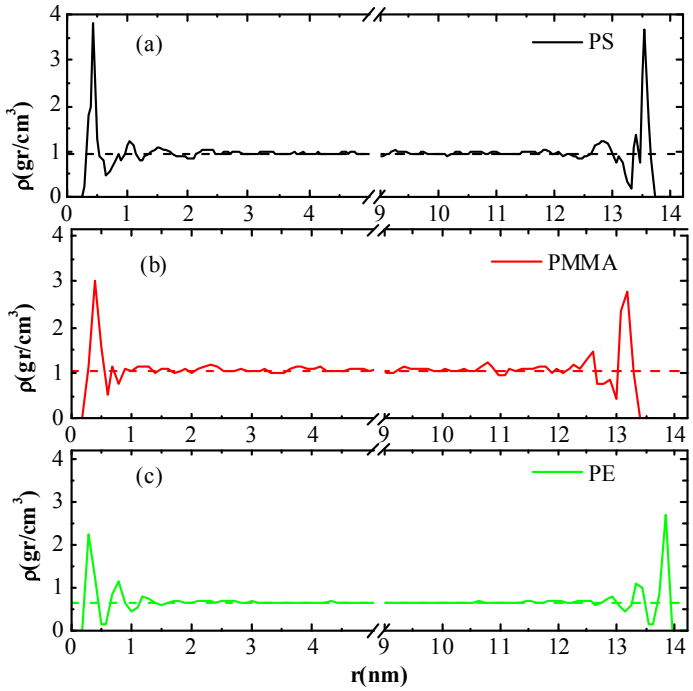

Figure 2. Monomer density profiles as a function of distance from graphene layers for **a)** PS, **b)** PMMA and **c)** PE, hybrid polymer/graphene systems. Bulk system's density is represented by a dashed horizontal line in all cases.

In order to extract information for the conformations of the polymer chains close to the surface we calculate the second rank bond order parameter, $P_2(\cos\theta)$, defined as: $P_2(\cos\theta)=\frac{3}{2}\langle\cos^2\theta\rangle-\frac{1}{2}$ where, θ is the angle between an arbitrary vector, which is defined along the molecule, and one Cartesian axis. This quantity provides information

about the orientation of individual parts of the polymer chain. In this work, we define a characteristic vector along the backbone of the polymer chain ($\boldsymbol{v}^{bb}$), for each polymer, which connects one carbon atom to the next not consecutive carbon atom (1-3) and we calculate its angle with *z*-axis (normal to the surface).

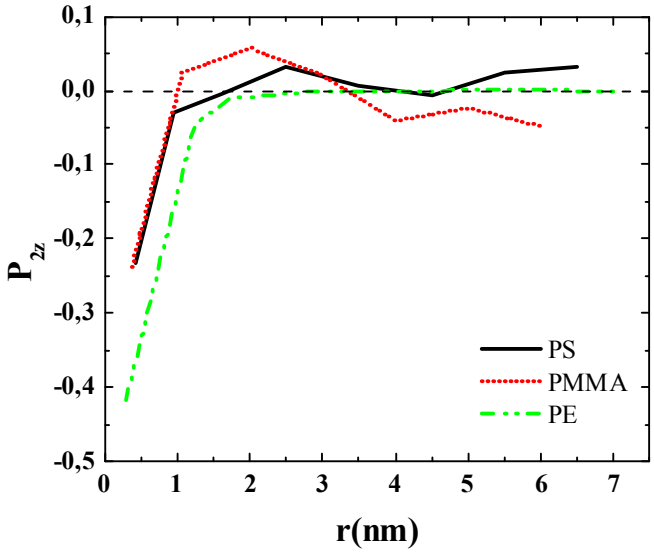

Figure 3. Bond order parameter $P_2(\cos\theta)$ along *z*-axis as a function of distance from graphene layer for a vector defined along the backbone in each of the three systems.

In Figure 3 $P_2(\cos\theta)$ has been analyzed as a function of the distance from the surface. Note that the data have been averaged over the equal distances from the two graphene layers in order to improve statistics, utilizing system's symmetry. $P_2(\cos\theta)$= *-0.5* signifies a vector with orientation parallel to surface, $P_2(\cos\theta)$=*1.0* normal to the surface, and $P_2(\cos\theta)$=*0.0* random orientation with respect to the surface. $P_2(\cos\theta)$ values denote an orientation almost parallel to the surface close to the graphene layer, which is gradually becomes random as the distance from the graphene increases. This behavior is common for the three systems, though more pronounced for PE. This is directly related to the layered structure, which has been observed in the density profile of PE.

Finally, we present a brief discussion for the dynamics of the hybrid interfacial systems. Dynamics in the segmental level can be studied through the calculation of the second-order bond order parameter as a function of time: $P_2(t)=\frac{3}{2}\langle\cos^2\theta(t)\rangle-\frac{1}{2}$ for the characteristic $\boldsymbol{v}^{bb}$ vector, which has been described previously. In this formula, *θ(t)* is the angle of the vector under consideration at time *t* relative to its position at *t=0*. We examine the average dynamics over the entire film. In Figure 4 the time autocorrelation functions of

$\boldsymbol{v}^{bb}$ characteristic vector is presented, for the three systems. A considerable difference in the relaxation time of the PE compared to the other two polymers is observed. $\boldsymbol{v}^{bb}$ characteristic vector is fully decorrelated after just *1ns*, whereas the time autocorrelation functions for the other two polymers have significant values at that time. Such differences in the mobility of the different polymers are not surprising if we consider the combinatory effect of both different interactions and different T_g values on the local polymer relaxation times. Moreover, the confined systems have slower dynamics than the respective bulk ones.

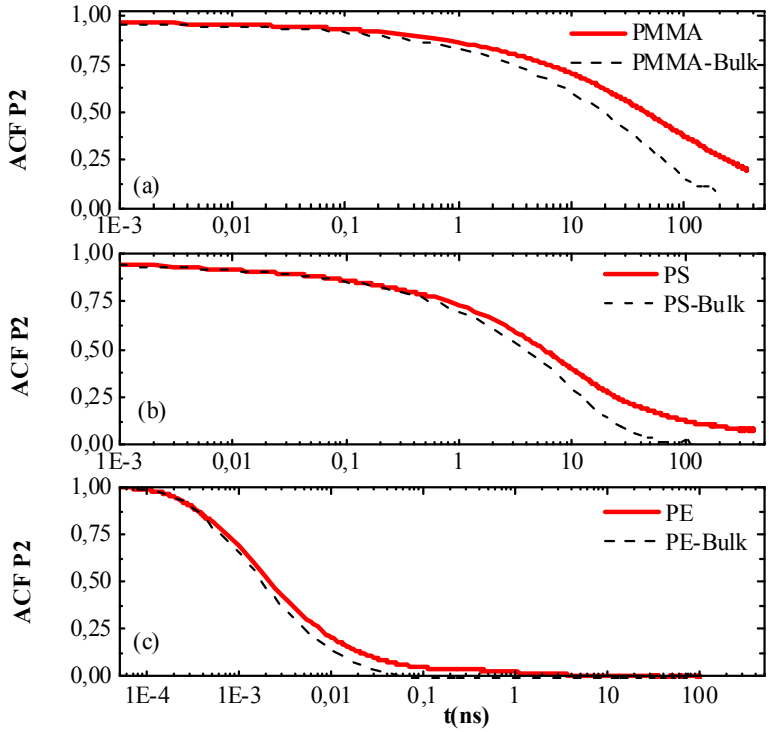

Figure 4. The autocorrelation functions of P_2 for the backbone characteristic vector ($\boldsymbol{v}^{bb}$) for the three hybrid polymer/graphene systems

To further quantify the differences in dynamics among the three systems we calculate the segmental relaxation times defined as, $\tau_{segm.} = \frac{\tau_{KWW}}{\beta}\Gamma\left(\frac{1}{\beta}\right)$ where τ_{KWW} is the relaxation time, which is extracted from a fitting of $P_2(t)$, with a stretch exponential function[20] (Kohlrausch-Williams-Watts, (KWW)): $P_2(t) = A\exp\left[-\left(\frac{t}{\tau_{KWW}}\right)^{\beta}\right]$ and β is the stretch exponent, which takes into account the deviation from the ideal Debye behavior (β=1). Segmental relaxation times τ_{seg} for all hybrid and bulk polymer model systems studied here, are shown in the last column of Table 1. It is clear that for all systems the

dynamics of the hybrid systems is slower, with a factor of *2* for PE, to about 3 for PS and up to *4* for PMMA, than the corresponding bulk ones. Note here, that the ratios of τ_{seg} of the hybrid over the τ_{seg} of the corresponding bulk system reveal the effect of different polymer/surface interactions on polymer dynamics. Furthermore, the dynamics of PE is much faster (about *4-5* orders of magnitude) than the relaxation of both PS and PMMA, while the relaxation time of PMMA chains is about *10* times slower than the one of PS. Finally, we have to mention that segmental relaxation times can be extracted through different vectors within the polymer chain, something which is also apparent among various experimental techniques. Here we chose $\boldsymbol{\nu}^{bb}$ characteristic vector, while a further analysis, where more vectors have been studied, and a comparison among different segmental relaxation times has been made, is presented in our recent publications.[19,21]

Conclusions

The current work presents a comparative study of three different polymer/graphene nanocomposites through detailed atomistic simulations. We performed atomistic molecular dynamics simulations on three different polymer/graphene interfacial systems, using polystyrene (PS), poly(methyl methacrylate) (PMMA) and polyethylene (PE) polymers. Our focus was on the structural conformational and dynamical properties of the polymer chains and the way that they diversify form their corresponding bulk behavior, as a function of the distance form the graphene layer. The three polymer films are almost of the same thickness. The radius of gyration, R_g and the end-to end vector, R_{ee}, are measures of the mean size and the extension of the entire polymer chain respectively. For both quantities, the values for the confined systems are very close to the corresponding bulk values. The density profiles of all three polymers highlight the attraction between the graphene layer and the polymer chains and display a symmetric shape with respect to the center of the film. The bulk density value is attained away from the surface, for each polymer respectively. Furthermore, quantitative differences are observed among the three polymers. The highest attraction from the graphene layer is observed for PS, then for PMMA and finally for PE polymer chains. Moreover, PE forms a well ordered layered structure close to the surface in contrast to the other two polymers.

The orientation of the segments of the polymer chains close to the surface is quantified by the calculation of the second rank bond order parameter, $P_2(\cos\theta)$. An orientation almost parallel to the surface close to the graphene layer is observed, which is

gradually becoming random as the distance from the graphene increases. This behavior is more pronounced for PE polymer, something which is consistent with its layered structure.

Finally, information about the mobility of the three different polymers, and the way that the graphene layer affects them, is extracted from the calculation of the autocorrelation function of the second-order bond order parameter, $P_2(t)$, for a characteristic vector at the monomer level. PE is substantially faster than the other two polymers as it is revealed from a comparison of the autocorrelation functions of Figure 4 as well as from the calculation of the segmental relaxation time, τ_{segm} (Table 1). PS presents the second faster dynamics, while the slowest one is PMMA. A more detailed study on the structural, the conformational and the dynamical properties of PMMA/graphene interfacial systems, is presented in our recent publication[19], while a further study on dynamics of different polymer/graphene systems will be presented in a forthcoming publication (*Rissanou and Harmandaris to be submitted*).

[1] C. N. R Rao, A. K. Sood, K. S. Subrahmanyam, A. Govindaraj, *J. Mater. Chem*. **2009**, *19(17)*, 2457.
[2] Z. Stitalsky, D. Tasis, K. Papagelis, C. Galiotis, *Prog. Pol. Sci.* **2010**, *35*, 357.
[3] H. Kim, A. A. Abdala, C. W. Macosko*, Macromolecules* **2010**, *43*, 6515.
[4] S. J. Park, R. S. Ruoff, *Nat. Nanotechnol*. **2009**, *4*, 217.
[5] D. R. Dreyer, S. J. Park, C. W. Bielawski, R. S. Ruoff, *Chem. Soc. Rev.* **2010**, 39, 228.
[6] T. Ramanathan, A. A. Abdala, S. Stankovich, D. A. Dikin, M. Herrera-Alonso, R. D. Piner, D. H. Adamson, H. C. Schniepp, X. Chen, R. S. Ruoff et al., *Nat. Nanotechnol*. **2008**, *3*, 327.
[7] R. J. Young, L. Gong, I. A. Kinloch, I. Riaz, R. Jalil, K. S. Novoselov, *ACS Nano* **2011**, 5, 3079.
[8] K. C. Daoulas, V. A. Harmandaris, V. G. Mavrantzas, *Macromolecules* **2005**, *38*, 5780; *Macromolecules* **2005**, *38*, 5796.
[9] A. P. Awasthi, D. C. Lagoudas, D. C. Hammerand, *Modelling Simul. Mater. Sci. Eng.* **2009**, *17*, 015002-1 – 37.
[10] C. Lv, Q. Xue, D. Xia, M. Ma, J. Xie, H. Chen, *J. Phys. Chem. C* **2010**, *114*, 6588.
[11] V. Harmandaris, K. Kremer, *Macromolecules* **2009**, *42*, 791; . *Soft Matter* **2009**, *5*, 3920.
[12] V. Harmandaris, C. Baig, *Macromolecules* **2010**, *43*, 3156.
[13] K. Johnston, V. Harmandaris, *Soft Matter* **2013**, DOI: 10.1039/c3sm50330e.
[14] B. Hess, C. Kutzner, D. van der Spoel, E. Lindahl,, *Journal of Chemical Theory and Computation*, **2008**, *4*, 435.
[15] W. L. Jorgensen, D. S. Maxwell, J. Tirado-Rives, *J. Am. Chem. Soc.* **1996**, *118*, 11225.
[16] M. G. Martin, J. I. Siepmann*, J. Phys. Chem. B* **1998**, *102*, 2569.
[17] W. A. Steele, *Surf. Sci.* **1973**, *36*, 317.
[18] J. Koo, *Polymer Nanocomposites Processing, Characterization, And Applications* **2006**, McGraw-Hill.
[19] A. N. Rissanou, V. Harmandaris, *Journal of Nanoparticle Research* **2013**, *15*, 1589:1-14.
[20] G. Williams, D. C. Watts, *Transactions from the Faraday Society* **1970**, *66*, 80.
[21] V. A. Harmandaris, G. Floudas, K. Kremer, *Macromolecules* **2011**, *44*, 393.